Inherent features in the growth of perylene crystals on an oil substrate

Xiangdong Liu* and Matthias Wuttig
I. Physikalisches Institut, RWTH-Aachen, 52056 Aachen, Germany
(Received 22 September 2005; revised manuscript received 30 November 2005; published 13 January 2006)

Inherent growth features for molecular crystals have been discovered by vapor-phase deposition of perylene molecules onto a liquid film. We have observed a unidirectional anisotropy in the growth of needle crystals, which indicates different accommodation probabilities at opposite steps. This observation shows that the extended and generally anisotropic molecular shape will introduce important steric effects on crystal growth which are absent from inorganic crystal growth. We have also observed a creased growth morphology for square crystals. Step interactions have been proposed as the possible mechanism of the creased growth.

DOI: 10.1103/PhysRevB.73.033405 PACS number(s): 68.35.Gy, 68.03.Fg, 68.55.Ac

The present and potential applications of organic crystals and thin films for electronic[1] and light emitting devices[2] drive strong interest in the fundamental understanding of the growth of organic crystals and thin films.[3] In contrast to the strong atomic bonding in inorganic crystals, in organic, molecular crystals, molecules are bound together by the relatively weak van der Waals forces. Furthermore, organic molecules possess extended, generally anisotropic shapes, which would introduce specific steric effects on crystal growth. Therefore, one would expect different growth behavior for organic crystals. On the other hand, as compared with the rich knowledge about conventional inorganic systems, there is up to now only limited understanding of the growth mechanisms of organic systems. In this work, we have discovered some new features of molecular crystal growth using α-perylene as prototype. We have observed a unidirectional anisotropy in the growth of needle crystals, indicating different accommodation probabilities at opposite steps. The differences in accommodation originate from the specific molecular shape and molecular orientation. This is contrasted with inorganic crystals where the atoms or ions can be treated as isotropic balls. We have also observed a creased growth morphology for square crystals. We ascribe the creased growth to step interactions, though we have no direct evidence for it. The revealed effects are based on the distinctive properties of molecular crystals and thus are expected to be shared by other molecular crystals.

Perylene was deposited from a shutter-controlled evaporator onto a liquid substrate of silicone oil (pentaphenyltrimethyltrisiloxane) at room temperature (RT).[4] The transparent, low-vapor-pressure silicone oil, which was spin-coated onto a polycarbonate plate prior to deposition, also served as a window of the vacuum system. An optical microscope with charge-coupled device (CCD) camera was focused onto the oil-vacuum interface, where crystal nucleation and growth took place. The deposition rate was calibrated by a quartz crystal microbalance mounted at the position of the sample. The average thickness of the oil film was determined by weighting with a microbalance. The solubility limit c_0 of perylene in silicon oil at RT was determined to be $0.5\pm0.05\%$ in volume. The normalized perylene concentration in the oil film $\sigma=c/c_0$ is calculated on the basis of the known c_0. In order to gain information about the crystal orientation, x-ray microdiffraction of individual crystals was carried out using Stoe IPDS-I diffractometers.

Perylene is a planar hydrocarbon with a formula of $C_{20}H_{12}$ [see Fig. 1(a)]. In the present experiments perylene crystallized in the α phase,[5] which has a centrosymmetric monoclinic crystal structure with paired molecules [compare Fig. 1(b)]. The unit cell of α-perylene with the space group $P2_1/a$ is defined by $a=11.35$ Å, $b=10.87$ Å, $c=10.31$ Å, and $\beta=\angle ca=100.8°$. Figure 1(b) shows a schematic top view of the unit cell of α-perylene. The molecular long axis L forms an angle of 83.3° with the a axis while it is almost perpendicular to the b axis (89.2°).

Figures 2(a)–2(c) show the typical growth shapes at various normalized concentrations. We find that the nucleation of perylene crystals invariably takes place at the oil-vacuum interface, and that nucleation occurs even at a normalized perylene concentration much less than unit. These give evidence that a significant concentration gradient exists in the oil film due to the slow diffusion of perylene molecules. However, we cannot exclude another possibility that the oil-vacuum interface is the preferential position for perylene molecules. The incubation period is generally observed for

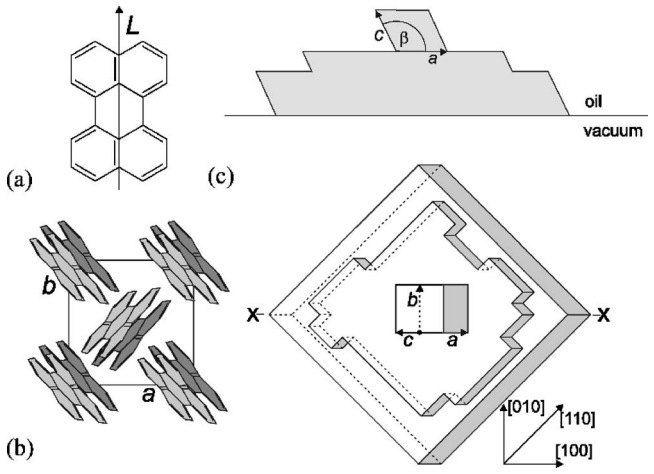

FIG. 1. (a) Molecular structure of perylene. The molecular long axis L is indicated. (b) Schematic sketch of an α-perylene unit cell projected onto the ab plane. (c) Schematic sketch of a platelet α-perylene crystal with a kinked growth step in the oil surface. The unit cell is superimposed on the crystal (see text). Lower panel: view of the platelet from the oil film side as seen during imaging; upper panel: cross section of the platelet crystal along xx as indicated in the lower panel.

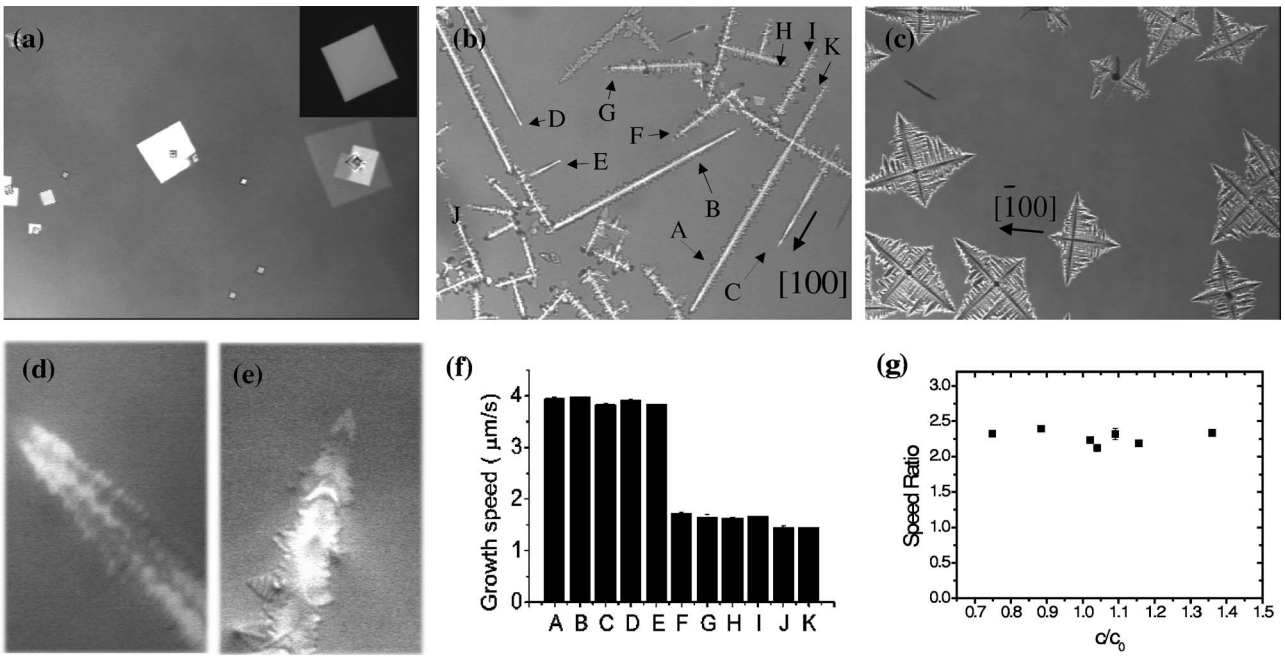

FIG. 2. (a)-(c) Growth shapes resulting after a short deposition interval (5-30 s) with a deposition rate of 68 Å/s. The resulting normalized perylene concentrations in the 20 μm thick oil films are (a) σ=0.34, (b) σ=1.36, and (c) σ=2.04. All images have a size of 800 μm$\times$600 μm; the inset in (a) shows a 120 μm$\times$120 μm square crystal under polarized light microscopy. For the growth of needle crystals as shown in (b), two well-distinguished steady-state growth speeds were observed. The growth speeds of the needle crystals specified in (b) are plotted in (f). The growth tips associated with the fast-growing and the slow-growing needles are shown in (d) and (e) (37 μm$\times$55 μm), respectively. In (b) and (c), for a few crystals the [100] or [$\bar{1}$00] direction is indicated by black arrows. (g) The ratio of two kinds of growth speeds keeps almost constant within a wide range of normalized concentration. Images shown in (a)-(e) are adopted from Ref. 6.

the nucleation. At a deposition rate of 68 Å/s, for example, the first nucleation is observed in 10–20 s since starting the deposition. With increasing perylene concentration, the growth shape evolves from square crystal [Fig. 2(a)], to needle crystal [Fig. 2(b)], and finally to dendrite [Fig. 2(c)].[7,8] For square crystals, the growth lasts for 10 min after stopping the deposition while the growth speed gradually decreases with time. For needle crystals and dendrites, the growth speed keeps constant after the deposition until the tip approaches to another crystal. These observations again show that the diffusion length of perylene molecule in the oil is quite small.

In the following, we will first focus on the growth of needle crystals, for which the growth speeds are surprisingly found to be distinctively different between the [100] and [$\bar{1}$00] direction. As an example, the growth speeds of a number of needle crystals specified in Fig. 2(b) have been measured and plotted in Fig. 2(f). The fast-growing direction was determined to be the [100] direction. A ratio of about 2.3 has been measured for the growth speed in the [100] direction to that in the [$\bar{1}$00] direction. More interestingly, this ratio does not depend on the perylene concentration within the concentration range where needle crystals are formed, as is seen in Fig. 2(g), though the growth speeds themselves change with the concentration. Corresponding to the different growth speeds, the growth tip also shows obvious discrepancy. The [100]-direction growing tip is corrugated [Fig. 2(d)] while the [$\bar{1}$00]-direction growing tip is relatively flat. All these observations indicate a unidirectional anisotropy in the $\langle 100 \rangle$-directional growth of perylene needle crystals in the oil surface. This asymmetric growth is also indicated by the unequal length of the $\langle 100 \rangle$-directional branches in dendrite growth [Fig. 2(c)]. Additional evidence can be found elsewhere.[6]

In a homogeneous environment for a crystal with an inversion center—such as α-perylene—growth in opposing directions must be equivalent with identical growth speed. Therefore the observed asymmetric growth can only originate from the break of symmetry of the environment. For the present case in which perylene crystals grow in the oil surface and perylene molecules are incorporated into the kinks directly from the oil, the existence of the oil-vacuum interface and the crystal growth confined by it break the inversion symmetry and are in fact the origin of the unidirectional growth anisotropy. The actual origin of symmetry breaking can be inferred from Fig. 1(c). It is apparent that the unit cell forms a blunt, monoclinic angle (β=100.8°) with the oil surface along the [100] direction, while it forms a sharp angle (79.2°) along the [$\bar{1}$00] direction. At the same time, the molecular long axis forms an angle of 96.3° (83.7°) with [100] ([$\bar{1}$00]) direction. Since the growth is confined in the oil film and a large concentration gradient exists, growth steps are formed only on one side of the platelet (oil side), and hence open kinks and steps are only present in the [100] direction, while closed kinks and steps in the [$\bar{1}$00] direction (see Fig. 1). Incorporation of perylene molecules with their

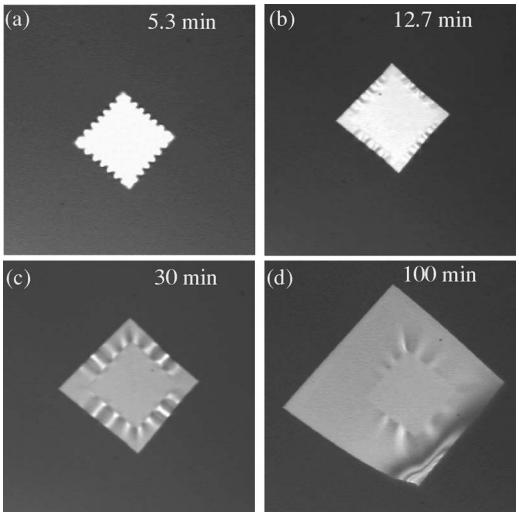

FIG. 3. The development and relaxation of the creases. The times counted from the new evaporation are labeled on the right top of the images. See text for details. All images have a size of 420 μm $\times$ 420 μm.

complex steric requirements into the open kinks can be supposed to be easier and thus to occur more frequently,[9] leading to a faster growth in the [100] direction. This scenario is supported by the independence of the speed ratio with respect to the supersaturation [Fig. 2(g)]. Therefore the observed asymmetric growth actually reflects the additional complexities in the growth of organic crystals which are induced by the finite molecular size and the complex molecular shape. Based on this finding, it is suggested that for molecular crystals, a steric factor should be introduced into the expression for the capture factor for the nucleation and that of the kinetic coefficient for the growth.

Now we turn our attention to the growth of square crystals. In this case, we observed an interesting creased growth morphology under certain conditions. As the first example, the creased morphology develops on a ready-grown square crystal upon increasing the evaporation rate. Figure 3 illustrates a typical observation. In this experiment, perylene had first been evaporated at a rate of 1.7 Å/s for 330 s onto a 30 μm thick silicone oil film, leading to the formation of a number of thin, square crystals. Three hours later, the growth stopped, then a new evaporation of 120 s was added using the same deposition rate. From this time on, the crystal started to grow into a creased shape. The creasing amplitude

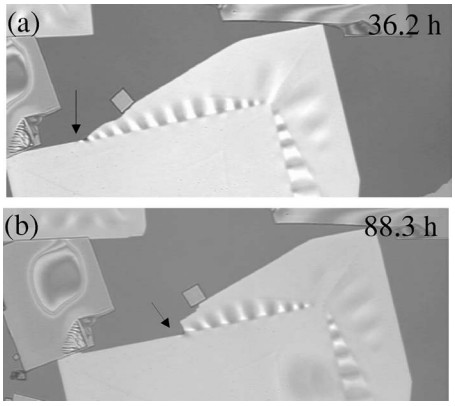

FIG. 4. The metastability of the creased crystal is shown by the redissolution of the creased part while the flat part remains. The images were recorded in 36.2 and 88.3 h after the second evaporation stopped.

at the growth front diminished with time and finally a flat and smooth growth front was restored. At the same time, the already formed creases also relaxed with time (Fig. 3). About 2 h later, the whole crystal became flat and no trace of creased growth was left. The creased shape can be recurred by a new evaporation.

In order to characterize the geometric properties of the creases, observations have been made upon positioning the crystal up and down around the focal plane of the microscopy. When the crystal was moved slightly away from the focal plane, a regular, sawtoothlike pattern was observed around the crystal edges [Fig. 3(a)]. The bright, round teeth exchanged their positions with the initial dark indentations after the crystal was moved from one side of the focal plane to the other side. When the crystal was just at the focal plane, straight edges were observed [Fig. 3(b)]. Crystals with such creases have also been taken out of the chamber so that the other side of the crystal can be imaged. By comparing the images from both sides of the same creased crystal, we can conclude that the observed is a creased morphology.

It is important to notice that only the part grown after the new deposition is creased [see Figs. 3(c) and 4]. This observation indicates that the formation of the creases is closely linked to the growth procedure. The creased crystals have been proven to be metastable. Figure 4 shows how the creased part redissolves while the old part remains.

The creases in the crystals have also been observed under continuous, slow evaporation. Under such a condition, the

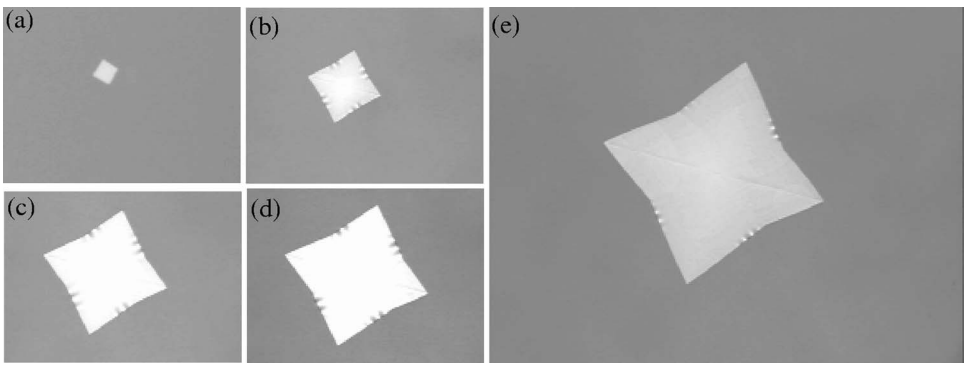

FIG. 5. Creases appear at the middle of the crystal edges when the crystal shape is changed from square into tetragon under continuous small flux.

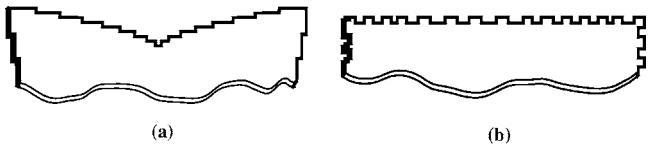

FIG. 6. Schematic sketches of the step distribution for a thin square crystal growing at (a) small supersaturation and (b) large supersaturation.

crystal is initially grown in square platelets, then gradually evolves its shape into a tetragonal one. Creases are observed and only observed when the straight edges of the square crystal are inwardly curved upon growth. Furthermore, the creases are only located within a narrow zone at the middle of each edge (Fig. 5).

Without finding an effective experimental method to directly explore the mechanism of the creased growth, we can just speculate on the possible one. We find that, by introducing elastic interactions between steps and assuming a resultant creased growth morphology from attractive interaction between neighboring steps, all the observations concerning the creases can be plausibly explained. Based on the elastic theory of continuous media, Marchenk and Parshin (MP) have predicted a repulsive elastic interaction between identical steps and an attractive one between opposite steps.[10] The MP law has been confirmed by a number of experiments with inorganic crystals.[11] Since the long-range interactions play particular roles for surface relaxation,[12] the elastic interaction between steps should also be valid for molecular crystals due to the long-range property of van der Waals forces. Keeping these in mind, we return to the creased morphology induced by a consecutive fast evaporation (Fig. 3). In this case, the supersaturation increased dramatically after a new evaporation (notice that the solution is already saturated before the evaporation), incurring a sudden increase in step density as schematically shown in Fig. 6(b). The attractive interaction between neighboring steps results in a compressive stress in the growth front and consequently produces the creased growth morphology. The situation is quite different under continuous, slow evaporation (Fig. 5). Under such a condition, the supersaturation remains small, and the nucleation of the growth steps only takes place at the corners due to the smaller nucleation energy and larger concentration there.[9,13] Therefore the crystals keep the square shape until a critical size, at which the time interval between two consecutive nucleation events at a corner is equal to the time required for the completion of the layer growth. Afterwards, steps start to accumulate as indicated by the gradually curved crystal edges. Since the concentration is large around the corners and small at the middle of the edges, the step propagation velocity decreases on its departure from the corners, and hence the step density is maximum at the middle of edges. At the same time, the opposite neighboring steps are only dynamically located around the midpoint of the edges [see Fig. 6(a)]. These explain the creases shown in Fig. 5. The interacted steps are always located at the growth front, and they dynamically move on with growth. This explains the metastability of creases. In the scenario of step interaction, the different tip structures observed for needle crystals [Figs. 2(d) and 3(e)] can also be explained. Considering that the step nucleation energy is the same for the two types of tips, the [100]-direction growing tip should have a larger step nucleation rate due to the more favorable steric condition for molecule accommodation. A larger nucleation rate means a larger step density and hence a stronger step interaction. Therefore the fast-growing tip shows a creased tip structure.

In summary, we have observed a unidirectional growth anisotropy and a creased growth morphology for perylene crystals in oil surface. The former illuminates the importance of the steric effects in the growth of molecular crystal, and the latter is possibly induced by step interaction. We would like to point out that the effects revealed in this work in principle also work in the growth of other molecular films.

We thank Professor Th. Michely for the permission to use his equipment and helpful discussions, and Dr. V. Kaiser for the x-ray microdiffraction measurements.

*Electronic address: xiang@physik.rwth-aachen.de

[1] H. Klauk and T. Jackson, Solid State Technol. **43**, 63 (2000).
[2] J. R. Sheats, H. Antoniadis, M. Hueschen, W. Leonard, J. Miller, R. Moon, D. Roitman, and A. Stocking, Science **273**, 884 (1996).
[3] For example, M. Voigt, S. Dorsfeld, A. Volz, and M. Sokolowski, Phys. Rev. Lett. **91**, 026103 (2003).
[4] G.-X. Ye, T. Michely, V. Weidenhof, I. Friedrich, and M. Wuttig, Phys. Rev. Lett. **81**, 622 (1998).
[5] D. M. Donaldson, J. M. Robertson, F.R.S., and J. G. White, Proc. R. Soc. London, Ser. A **220**, 311 (1953); A. Camerman and J. Trotter, *ibid.* **279**, 129 (1964).
[6] X. Liu, V. Kaiser, M. Wuttig, and T. Michely, J. Cryst. Growth **269**, 542 (2004).
[7] E. Ben-Jacob and P. Garik, Nature **343**, 523 (1990).
[8] J. S. Langer, Rev. Mod. Phys. **52**, 1 (1980).
[9] A. A. Chernov, Kristallografiya **8**, 87 (1963).
[10] V. I. Marchenko and A. Ya. Parshin, Sov. Phys. JETP **52**, 129 (1980).
[11] M. Giesen, Prog. Surf. Sci. **68**, 1 (2001).
[12] A. Pimpinelli and J. Villain, *Physics of Crystal Growth* (Cambridge University Press, Cambridge, England, 1997).
[13] W. W. Mullins and R. F. Sekerka, J. Appl. Phys. **34**, 323 (1963).